

Alexander Clement, Wolfgang Koch, Birgit Glasmacher, Gerhard Pohlmann*

Droplet sizes and delivery rates from film breakup aerosolisation mode in porous materials

<https://doi.org/10.1515/cdbme-2024-2040>

Abstract: A novel two-phase aerosolisation mode utilizing porous materials is investigated, aiming to improve aerosol delivery for medical inhalation. Sintered stainless steel filters with varied pore sizes (PS) from 0.2 μm to 7 μm were used to generate aerosols from a 0.9 wt.% sodium chloride solution. Droplet sizes and delivery rates were measured using laser diffraction spectroscopy. Further measurements included shadow imaging. Results indicate that aerosolisation occurs within a specific range of PS with droplet sizes increasing with increasing PS. The droplets generated are suitable for inhalation therapies. A hypothesis is established about the process of droplet formation which states that different PS within the porous material serve distinct functions that contribute to the breakup of liquid films into aerosol particles. Droplet formation is the result of film breakup in pores filled with fluid. This low-energy aerosolisation method has the potential to be used in handheld devices for sensitive drug formulations, overcoming the limitations of current technologies. Further research is needed to optimize the pore size distribution and enhance aerosol generation efficiency.

Keywords: Porous Materials, Aerosolisation, Droplet Sizes, Aerosol Delivery Rate, Film Breakup

1 Introduction

Two-phase aerosolisation uses a gas to aerosolise a fluid into small droplets. It is an established procedure for generating aerosols for medical inhalation [1]. Inhalation therapy can be

used for example to deliver bronchodilators to asthma patients or insulin to diabetic patients. Droplet size is the most important parameter for the success of medical inhalation therapies. Furthermore, the delivery rate and the efficiency of the aerosolisation process are key parameters. The pharmaceuticals developed nowadays often consist of formulations, which are sensitive to shear forces and high temperatures [2]. This makes an efficient, low energy aerosolisation process necessary. The available handheld devices fulfil these requirements only partially [3]. These requirements can be met with two-phase aerosolisation.

There are two existing approaches in which porous material is used for the aerosolisation process. In an existing bioaerosol nebulizer, the Sparging Liquid Aerosol Generator (SLAG), the fluid to be nebulized is applied to the surface of the porous material in a disc-like shape and forms a liquid layer on the surface. The mass median diameter (MMD) of the particles generated is 0.89 μm [4]. The drawbacks are low efficiency, high energy input and complicated fluid control. The second approach, developed by Hazani, involves a proposal for a device which uses the porous material to nebulize the fluid by filling the material from upstream using less energy input [5]. The physical processes involved in this method are not yet understood. Investigating these processes could optimize the mode of operation and possibly reduce energy consumption while producing aerosol particles in the suitable range from 1 to 5 μm . Such a gentle aerosolisation mode would allow the use of porous materials in handheld devices.

In this study, the mode of operation for two-phase aerosolisation using sintered stainless steel porous materials (see Figure 1, left side) was investigated. Particle sizes were determined for different pore diameters and found to be suitable for medical inhalation. Further, a hypothesis for the breakup process was developed and supported by model calculations.

These findings suggest that optimizing this method could overcome the limitations of current aerosolisation devices, offering a low-energy solution suitable for handheld devices and sensitive formulations.

*Corresponding author: **Gerhard Pohlmann:** Fraunhofer Institute for Toxicology und Experimental Medicine (ITEM), Nikolai-Fuchs-Str. 1, 30625 Hannover, Germany, e-mail: gerhard.pohlmann@item.fraunhofer.de

Alexander Clement, Wolfgang Koch: Fraunhofer ITEM, Hannover, Germany

Birgit Glasmacher Institute for Multiphase Processes, An der Universität 1, Garbsen, Germany

2 Materials and Methods

2.1 Porous materials and test fluid

The porous materials used were sintered stainless steel filters with different nominal PS. The filters are of cylindrical beaker geometry (closed on one side). The cylinder is 20 mm high and 12.5 mm in diameter, all walls are 1.6 mm thick, having a material volume of 1277 mm³. Nominal PS used were 0.2, 0.5, 2, 7 and 15 μm (Art.-no. SS-4F-K4-02, -05, -2, -2 and -15, Swagelok Company). The minimum and maximum PS and the porosities for each nominal pore size are given in Table 1. The fluid used is a 0.9 wt.% sodium chloride solution (Prod.-no. A1671, AppliChem GmbH).

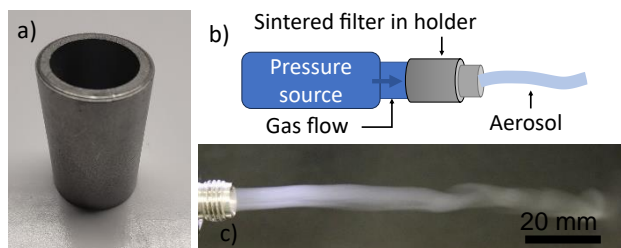


Figure 1: a) Sintered stainless steel filter in beaker shape, diameter 12.5 mm, height 20 mm; b) Aerosolisation setup; c) Generated aerosol from sintered filter in filter holder

Table 1: Nominal, minimum and maximum pore diameters of the sintered stainless steel filters

Nom. PS in μm	Min. PS in μm	Max. PS in μm	Porosity in %	Void volume in mm ³
0.2	na	na	30	380
0.5	0.5	2	24	306
2	1	4	38	489
7	5	10	39	500
15	11	25	na	na

2.2 Nebulizing process

For the measurements, the sintered filters are prepared by rinsing with demineralised water to remove sodium chloride particles from previous tests. The filters are then filled with 200 μl of 0.9 wt.% sodium chloride solution. For the experiments, the sintered filter is either attached to the end of the gas pressure source (surface observation) or placed into the designated holder (Art.-no.: SS-6TF-MM-05, Swagelok Company) in line with the pressure source. To start the nebulizing process, the pressure valve is operated manually and opened gradually until first aerosol particles emerge from the sinter filter. The applied pressure is in the range from 0.1

to 1 bar. Further adjustments are made to obtain an aerosol with the highest optical density.

The gas flow and pressure difference are measured using a Series 4043 flowmeter (TSI Instruments). To measure the delivery rate from the process, the filter holder is weighed every 30 s and the difference between the current and the previous weighing is calculated. Each PS is measured 4 times, the number of measurements depends on how long aerosolization is possible.

2.3 Shadow imaging

Shadow imaging is used in two setups to gain insights into the physical processes taking place at the surface of the sintered filter. In the first setup, the aerosol flow is observed from a perpendicular perspective imaging the side of the cylinder, in the second setup the camera is directed vertically on to the surface of the sintered filter. The high-speed camera used is set to a framerate of 7435 Hz. Attached to the camera is a K2 DistaMax Long distance microscope (Infinity Photo Optical Company) with the C2 objective, see Figure 2.

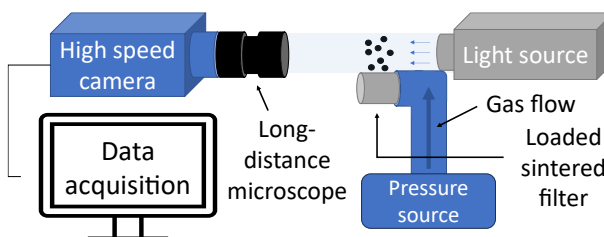


Figure 2: Shadow image setup

2.4 Particle size measurements

Particle sizes were measured using laser diffraction spectroscopy (Spraytec, Malvern Panalytical Ltd.). Five measurements were carried out for each of the five sinter filters tested. A 300 mm lens with a measurement range from 0.1 μm to 900 μm was used. The measurement results were filtered using two threshold criteria: the transmission had to be below 98%, and the calculated residual below 2%.

3 Results

3.1 Nebulizing process parameters measured

Aerosolisation is possible with nominal PS ranging from 0.2 μm to 7 μm , but not with a PS of 15 μm . The nebulizing

process for the investigated PS takes place at gas flow rates in the range from 0.1 l/min to 1.5 l/min. The aerosol delivery rates are given in Figure 3. The aerosolisation process starts only after a certain pressure threshold is reached. The smaller the nom. PS, the higher is the pressure threshold.

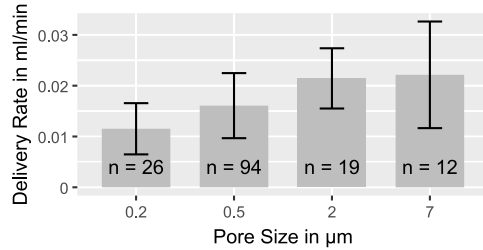


Figure 3: Measured values, standard deviation and number of measurements of the delivery rates.

3.2 Surface observation by shadow imaging and direct observation

The side view (see Figure 4) of the filter surface shows that the aerosol is only emitted at confined areas and not over the entire observed width of the cylinder side (8 mm). The velocity of the aerosol within the observed area ranges from 1 m/s to 10 m/s. In addition, bubbles with diameters between 0.2 mm and 0.25 mm are observed at the filter surface. These bubbles occur at irregular intervals, with their frequency estimated to be below 1 Hz.

In the top view (not shown), three distinct types of behaviour can be observed in the pores: no visual activity, slow activity, and fast activity. The slow activity is below 10 Hz, the fast activity occurs at frequencies between 500 Hz and 4000 Hz. The limited number of aerosolisation spots is also observed in the top view. Approximately 0.4 % of the pores are emitting an aerosol.

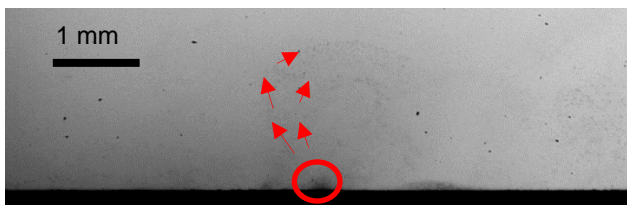


Figure 4: Shadow image of the surface of a sintered filter with nominal PS of 0.5 μm (black, at the bottom) and particles emerging from the filter. The red circle shows position of aerosolisation, red arrows indicate direction of particles.

3.3 Particle sizes vs. nominal pore size

The measured $Dv50$ median values range from 0.94 μm to 3.65 μm (see Figure 5). Particle sizes increase significantly

from 0.2 μm to 2 μm ; however, there is no significant change in particle sizes between 2 μm and 7 μm . The particle size does not change significantly with the gas flow rate (from 0.1 l/min to 1.5 l/min). The number of measurements per PS depends on how many measurements were filtered due to the quality criteria.

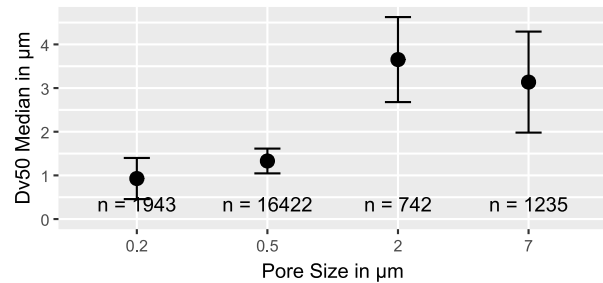


Figure 5: Measured $Dv50$ particle sizes with standard deviation (SD) and number of measurement points (n).

4 Discussion

Shadow imaging shows that only a limited number of pores contribute to the process. We hypothesize that the pores in the porous material have three functions. As the sintered stainless steel material consists of a pore size distribution, the functions must depend on the pore size.

The smaller the pores, the stronger the capillary force acting on the liquid. We therefore suggest that the smallest pores act as liquid reservoirs, visible in high-speed camera images as slow-moving areas, where water shifts due to pressure fluctuations but remains within the material. The pores with the largest diameter serve as gas channels. The medium-sized pores act as the aerosolizing pores. Pressure drop across the sinter filter shifts the sodium chloride solution into the downstream areas of the filter material. Pressure fluctuations within the porous material periodically shift small portions of liquid into the medium-sized pores. The displaced fluid forms a film inside the pore, blocking it. The gas flowing through this pore moves the film to the outer downstream area of the porous material, where the pores widen, the film diameter increases, and the film thickness decreases. Upon reaching a critical film thickness, the film breaks up into small droplets, forming an aerosol. This breakup model is depicted in Figure 6. There is a geometrical limitation that prevents aerosolisation above a nominal PS of 7 μm . Based on the hypothesis that films form inside the pores, we conclude that with increasing nominal PS, the fluid film inside the pores breaks up while still being thicker than in smaller pores. To support the hypothesis, the measured number of droplets generated per seconds is compared to the number of droplets

expected from the breakup model described. The number of droplets generated per second is calculated by weighing the gravimetrically measured delivery rates (see Figure 3) with the measured particle size distribution and derive the number of droplets per size range, which are then summed up.

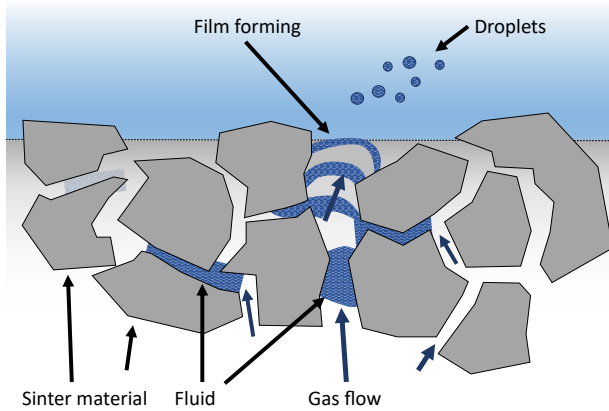


Figure 6: Breakup model for film breakup in porous materials. The interaction of gas and fluid inside of the porous material creates thin films which create an aerosol by breaking up.

The aerosol generation rate R_T , the number of particles generated per second, can be calculated using Eq. 1, where n_{pores} is the number of active pores, f_B is the film building frequency and $N_{droplets}$ is the number of droplets per film. Shadow imaging is used to determine the number of active pores and the film formation frequency. It is assumed that each active pore undergoes film breakup at the measured frequency and that the volume of the film (critical thickness multiplied by the film area and the constant t_{film}) breaks up into droplets with a volume corresponding to the MMD.

$$R_T = n_{pores} \cdot f_B \cdot N_{droplets} \quad (1)$$

The measured generation rates and the corresponding model predictions are displayed in Figure 7. The coefficient of determination (R^2) is 0.94, indicating that the model provides a strong fit to the measured data.

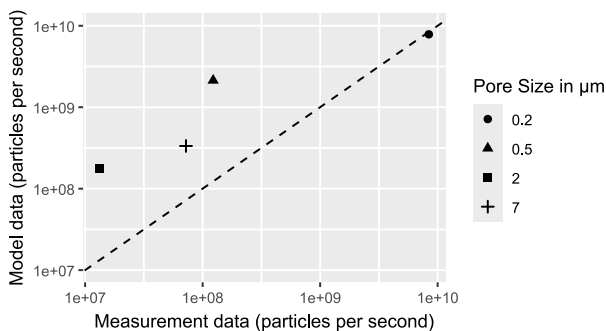


Figure 7: Comparison of measured values with model data. The coefficient of determination calculates to $R^2 = 0.94$.

An important finding is the possibility of influencing aerosol particle sizes by altering the nominal pore size. It is assumed that the pore size distribution has a significant influence on the process and should therefore be investigated further

Conclusion

The presented investigation provides basic insights into the physical processes of two-phase aerosolisation from porous materials. In the investigated processes, droplet sizes increase with larger pore diameters, and aerosolisation ceases beyond a certain pore size threshold. Using shadow imaging for qualitative insights and laser diffraction spectroscopy for quantitative data, a hypothesis for the aerosolisation process was established. The hypothesis posits that different PS in a pore size distribution serve different functions and that liquid films break up near the surface of the porous material. A comparison of measured droplet generation rates with model estimates further supports the hypothesis.

Transferring these findings to aerosolisation devices for medical inhalation requires further investigation of the breakup process in the active pores, as a significant portion of pores does not participate in the aerosolisation process. Nevertheless, aerosolisation employing a porous material shows promising results for nebulizing sensitive drug formulations in a mobile nebulizing device.

Author Statement

The authors state no funding involved. Authors state no conflict of interest.

References

- [1] Ali M.: Pulmonary Drug Delivery. In: Handbook of non-invasive drug delivery systems: Non-invasive and minimally-invasive drug delivery systems for pharmaceutical and personal care products (Editor: V. S. Kulkarni). Amsterdam: Elsevier, 2010, pp 209–246.
- [2] van Rijn, C.J.M., Vlaming, K.E., Bem, R.A. et al. Low energy nebulization preserves integrity of SARS-CoV-2 mRNA vaccines for respiratory delivery. Sci Rep 13, 8851 (2023).
- [3] Klein, D. M.; Poortinga, A.; Verhoeven, F. M.; Bonn, D.; Bonnet, S.; Rijn, Cees J. M. van: Degradation of lipid based drug delivery formulations during nebulization. Chemical Physics, 547 2021, p. 111192. doi:10.1016/j.chemphys.2021.
- [4] Alsved, M., Widell, A., Dahlin, H. et al.: Aerosolization and recovery of viable murine norovirus in an experimental setup. Scientific reports, 10 (1) 2020, p. 15941.
- [5] Hazani M.: Aerosol generating devices (WO 2020/003305 A1). 24.06.2019.